

A Compact Wideband Slot Antenna for Universal UHF RFID Reader

Waleed Abdelrahim and Quanyuan Feng*

Abstract—A compact wideband circularly polarized square slot antenna for universal UHF RFID reader applications is proposed and tested. An L-shaped radiator at lower surface of the substrate is used to feed the proposed antenna. To achieve a broadband circular polarization (CP) and good performance, two rectangular stubs with different sizes are inserted at opposite corners of the square slot at the upper surface of the substrate. A small rectangular slit is used to improve the impedance matching of the proposed antenna. The antenna's measured < 10 -dB impedance bandwidth and measured 3-dB axial ratio bandwidth are 70.2% (660–1374 MHz) and 45.8% (796–1269 MHz), respectively. The proposed antenna has a dual circular polarization characteristic, wide impedance bandwidth, wide axial ratio, compact size, and maximum measured gain about 3.9 dBi. The total size of the proposed antenna is $120 \times 120 \times 1.6$ mm³. Furthermore, the impedance bandwidth and axial ratio bandwidth of the proposed antenna cover the entire UHF RFID band easily. The proposed antenna is suitable for UHF RFID reader applications.

1. INTRODUCTION

Radio-frequency identification (RFID) is a technology that employs radio waves for exchanging data between tags and readers [1]. Recently, RFID technology in ultra-high frequency (UHF) band (840–960 MHz) has been widely used in several applications, including tracking, access control, etc. [2]. In practice, RFID tags are always randomly oriented, and in most cases, RFID tag antennas are linearly polarized (LP). Hence, the antenna of an RFID reader device is preferred to design with broadband circularly polarized (CP) wave to ensure the reliability of transferred information between reader and tag [3].

Globally, each country or region has its frequency band for UHF RFID applications. Consequently, a universal reader antenna with good performance in the whole UHF RFID band will be desired and useful for RFID system implementation and cost reduction [4, 5]. Several patch and architecture designs of reader antennas are reported to cover the entire UHF RFID band [6–8]. However, these reader antennas have large size, narrow impedance bandwidth and axial ratio bandwidth, and are challenging to design. Slot antennas have several merits including low cost, easy fabrication, simple structure, low profile, and broader impedance and circular polarization bandwidths [9]. Recently, several slot antenna designs have been proposed to cover the entire UHF RFID band [10, 11]. However, these antennas still have a relatively narrow impedance bandwidth and axial ratio (AR) bandwidths.

In this letter, we propose a wideband slot reader antenna for universal UHF RFID applications. The antenna comprises an L-shaped strip radiator on the ground plane and a square slot substrate with two rectangular shape strips placed at opposite corners of the square slot on the top side of the substrate. It is noted that the proposed antenna shows measured < 10 -dB reflection coefficient $|S_{11}|$ bandwidth of 70.2% (660–1374 MHz) and measured 3-dB axial ratio bandwidth of 45.8% (796–1269 MHz). Compared

Received 9 January 2018, Accepted 21 February 2018, Scheduled 9 March 2018

* Corresponding author: Quanyuan Feng (fengquanyuan@163.com).

The authors are with the School of Information Science and Technology, Southwest Jiaotong University, Chengdu, China.

to the above-mentioned reader antennas, the proposed antenna has a wider impedance bandwidth, wider axial ratio, and compact size. The overlapped bandwidth of the proposed antenna is 473 MHz (796–1269 MHz).

The remainder of this letter is organized as follows. The antenna configuration and parametric studies are presented in Section 2. Section 3 illustrates the antenna simulation and measurement results, and antenna performance comparison. A brief conclusion is demonstrated in Section 4.

2. ANTENNA DESIGN AND PARAMETRIC STUDIES

2.1. Antenna Structure

The configuration of the proposed antenna is shown in Figure 1. The antenna printed on an FR4 substrate ($\epsilon_r = 4.4$ and $\delta = 0.02$) with thickness of 1.6 mm. The dimensions of the proposed antenna are $120 \times 120 \times 1.6 \text{ mm}^3$. The proposed antenna consist of an L-shaped metal strip as radiator on the lower surface of the substrate and a square slot with two rectangular stubs placed at the opposite corners on the upper surface of the substrate. The L-shaped radiator is used to generate two resonant modes, and the combination of two resonant modes realizes a wideband frequency. Placing two rectangular stubs ($L_3 \times W_3$, $L_5 \times W_4$) at opposite corners is a common method to produce a circular polarization wave with different polarizations. Cutting a small rectangular slit at the left side rectangular stub ($L_5 \times W_4$) is used to improve the impedance matching of the proposed antenna. The dimensions of the proposed antenna in detail are shown in Table 1.

The proposed antenna evolution is illustrated in Figure 2. Four antennas (Antenna 1, Antenna 2, Antenna 3, and Antenna 4) are discussed here. Antenna 4 is the proposed antenna in this article. Antenna 1 is a square slot antenna with an L-shaped metal strip at lower centre of the slot. A rectangular stub ($L_5 \times W_4$) added at the lower left side of the slot to achieve Antenna 2. The AR bandwidth of Antenna 2 is still above 3-dB and has no circular polarization radiation. In Antenna 3, another rectangular stub ($L_3 \times W_3$) is added at the upper right side of the slot. The AR bandwidth

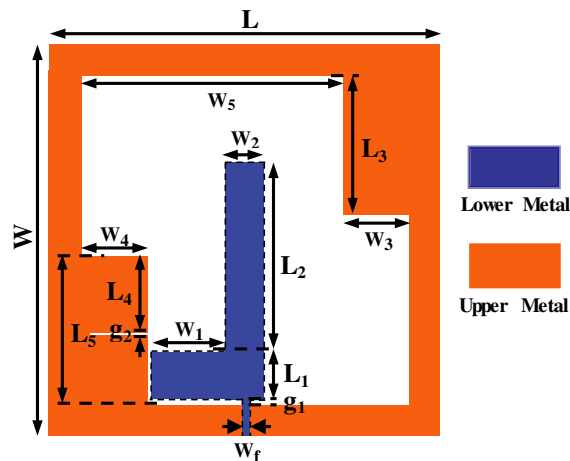


Figure 1. Geometry of the proposed antenna.

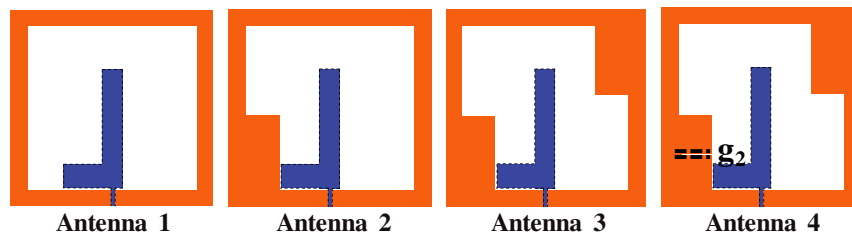


Figure 2. The proposed antenna evolution.

Table 1. Dimensions of proposed antenna (unit: mm).

L	L_3	W	W_3	W_f
120.0	42.0	120.0	20.0	2.0
L_1	L_4	W_1	W_4	g_1
15.0	23.5	23.0	20.0	1.0
L_2	L_5	W_2	W_5	g_2
58.0	45.0	12.0	80.0	0.5

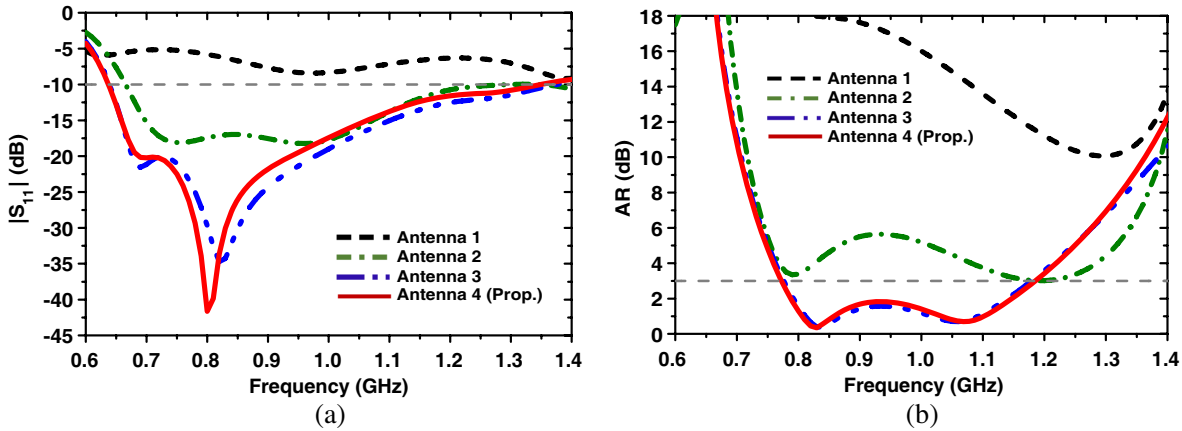


Figure 3. Simulated (a) reflection coefficient $|S_{11}|$ and (b) axial ratio (AR) responses for antenna 1, 2, 3, and antenna 4. Antenna 4 is the proposed antenna.

of Antenna 3 is below 3-dB. Antenna 3 has a good circular polarization characteristic due to the two rectangular stubs at opposite corners. To obtain Antenna 4, a small rectangular slit with width g_2 is etched at middle of the rectangular stub ($L_5 \times W_4$) at lower left side of the slot.

As can be seen from Figure 3, Antenna 1 has LP radiation. Antenna 2 generates two resonant frequency modes and has a good impedance matching. However, Antenna 2 still has no circular polarization radiation characteristics. Wide impedance bandwidth (from 637 MHz to 1370 MHz), wide axial ratio (from 775 MHz to 1180 MHz), and good impedance matching are achieved in Antenna 3. Antenna 4 has improvement in the impedance matching and a bit wider axial ratio (771–1188 MHz) bandwidth.

To explain the CP radiation on the proposed antenna, the simulated current distribution at 900 MHz is shown in Figure 4. The figure illustrates current directions on the L-shaped feedline and the square slot at four phase angles 0, 90, 180, and 270°, increasing by 90°. The current on the square slot and the feedline travels in clockwise direction, which results in left-hand circularly polarized (LHCP) radiation in the $+z$ direction. The right-hand circularly polarized (RHCP) radiation can be achieved by changing the positions of the two rectangular stubs to the other slot corners and changing the horizontal part of the L-shaped feedline from $-y$ -direction to the positive y -direction.

2.2. Parametric Studies

Figure 5 presents the influence of the width of the small slit (g_2) on the reflection coefficient $|S_{11}|$, axial ratio, and gain of the proposed antenna. As can be seen from Figure 5(a), the value of g_2 controls the resonant frequency of the proposed antenna reflection coefficient without influence on the start and end of the reflection coefficient bandwidth. When the value of g_2 increases, the resonant frequency of the reflection coefficient shifts toward the lower frequencies. The influences of g_2 on the axial ratio bandwidth and gain are shown in Figure 5(b) and Figure 5(c), respectively. The influences of g_2 on the axial ratio bandwidth and gain are inconsiderable.

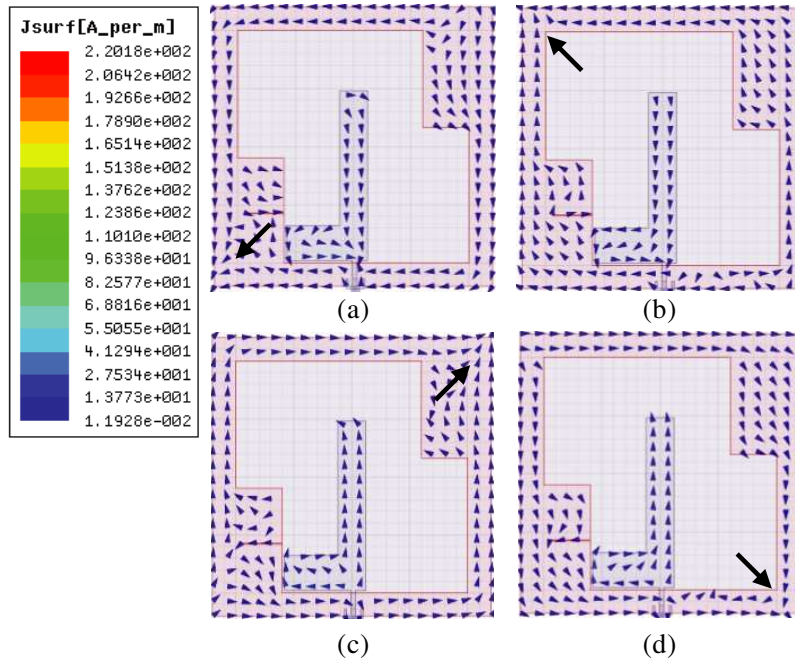


Figure 4. Surface current distribution of the proposed antenna at 900 MHz in the phase of (a) 0° , (b) 90° , (c) 180° , and (d) 270° .

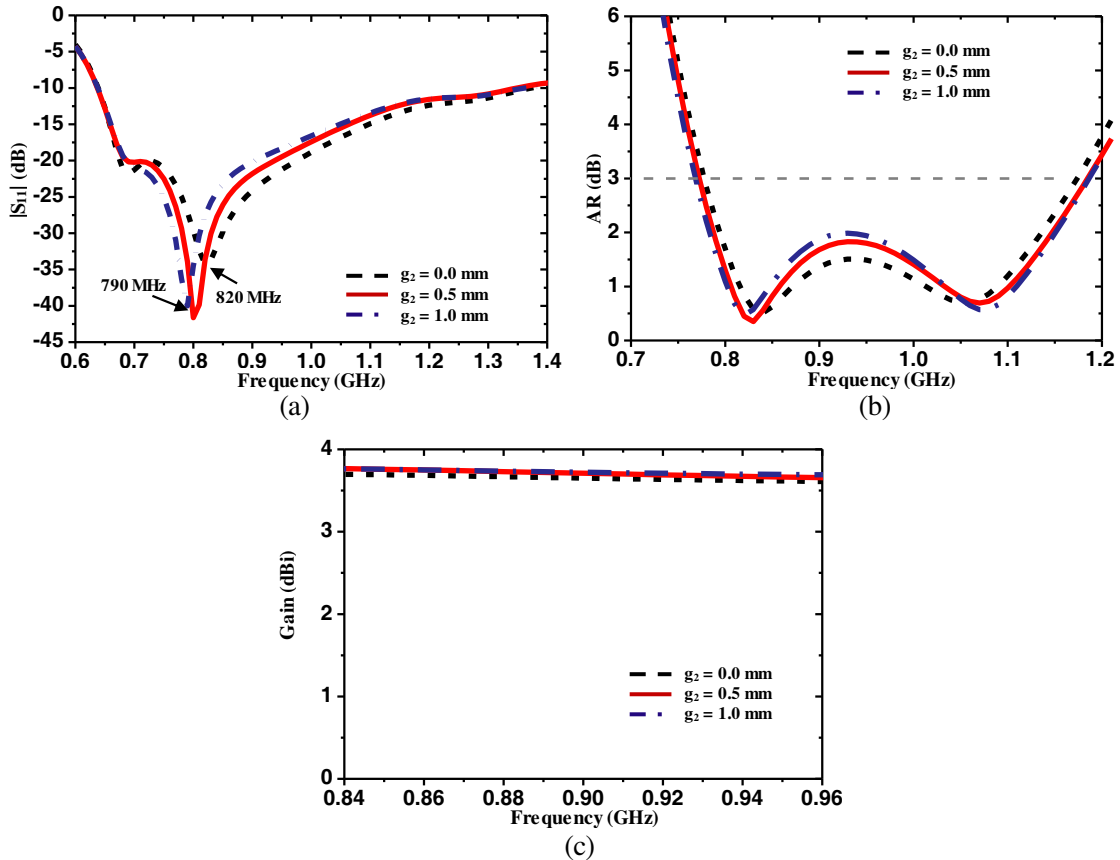


Figure 5. Simulated (a) reflection coefficient $|S_{11}|$, (b) axial ratio (AR) and (c) gain when g_2 is tuned.

The influences of width (W_4) of the rectangular stub ($L_5t \times W_4$) on the reflection coefficient $|S_{11}|$, axial ratio, and gain of the proposed antenna are shown in Figure 6. The influence of W_4 on the reflection coefficient is shown in Figure 6(a). When the value of W_4 increases, the end frequency of the reflection coefficient decreases toward the lower frequencies without influence on the start frequency of the reflection coefficient bandwidth. Figure 6(b) illustrates that when W_4 increases, the axial ratio band decreases toward the lower frequencies without influence on the start frequency of the axial ratio bandwidth. The influence of W_4 on the gain of the proposed antenna is demonstrated in Figure 6(c). The influence of W_4 on the gain is inconsiderable. Therefore, the end frequency of the reflection coefficient bandwidth and axial ratio bandwidth can be reconfigured easily by changing the value of width W_4 .

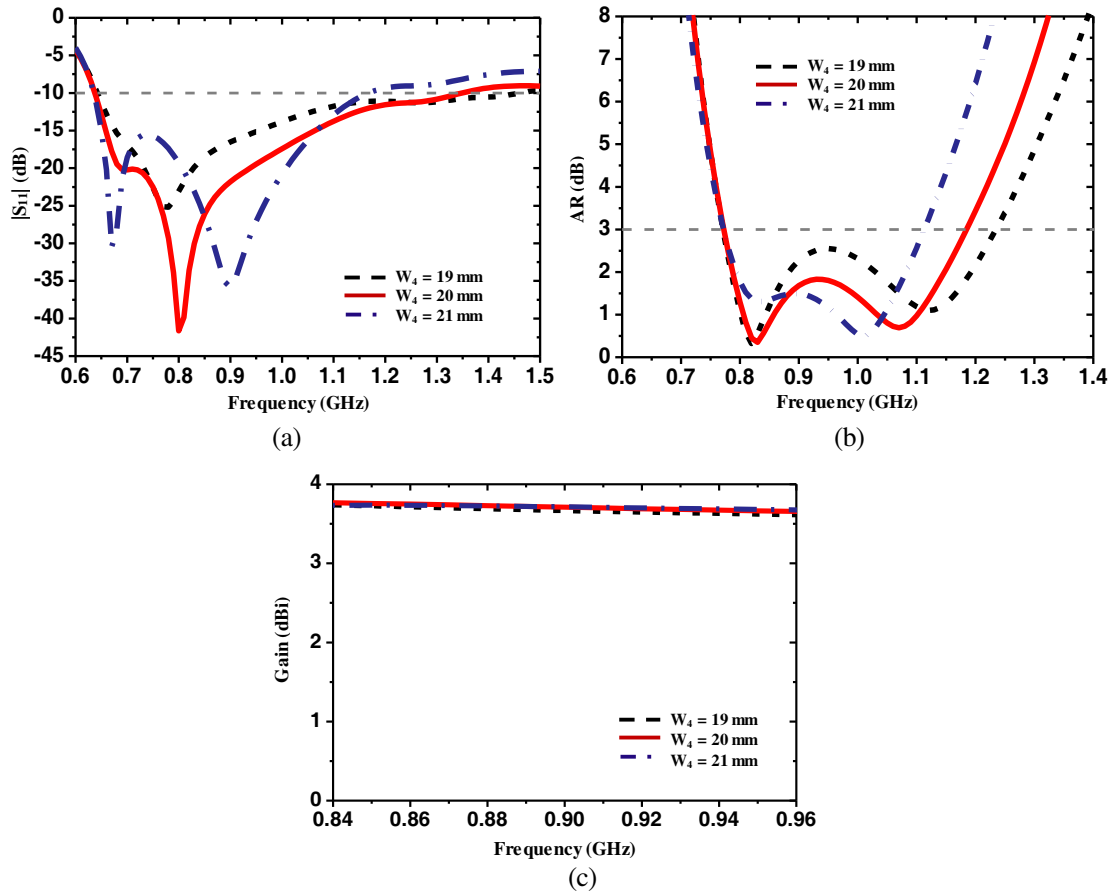


Figure 6. Simulated (a) reflection coefficient $|S_{11}|$, (b) axial ratio (AR) and (c) gain when W_4 is tuned.

3. SIMULATION AND MEASUREMENT RESULTS

The antenna's radiation patterns and reflection coefficient $|S_{11}|$ are measured using SATIMO measurement system and an Agilent E5071C vector network analyzer, respectively. Figure 7(a) shows a comparison between the simulated and measured reflection coefficients of the antenna. The simulated < 10 -dB reflection coefficient bandwidth is from 637 to 1343 MHz (706 MHz). The measured < 10 -dB reflection coefficient bandwidth is from 660 MHz to 1374 MHz (714 MHz). The measured reflection coefficient agrees well with the simulated one. Figure 7(b) shows the simulated and measured axial ratios of the antenna. The simulated 3-dB axial ratio is from 771 MHz to 1188 MHz (417 MHz) whereas the measured one is from 796 MHz to 1269 MHz (473 MHz). The measured axial ratio results are slightly shifted to higher frequency, and the experimental results generally agree well with the simulated ones. The slight frequency shift between the measured and simulated results can be attributed mostly

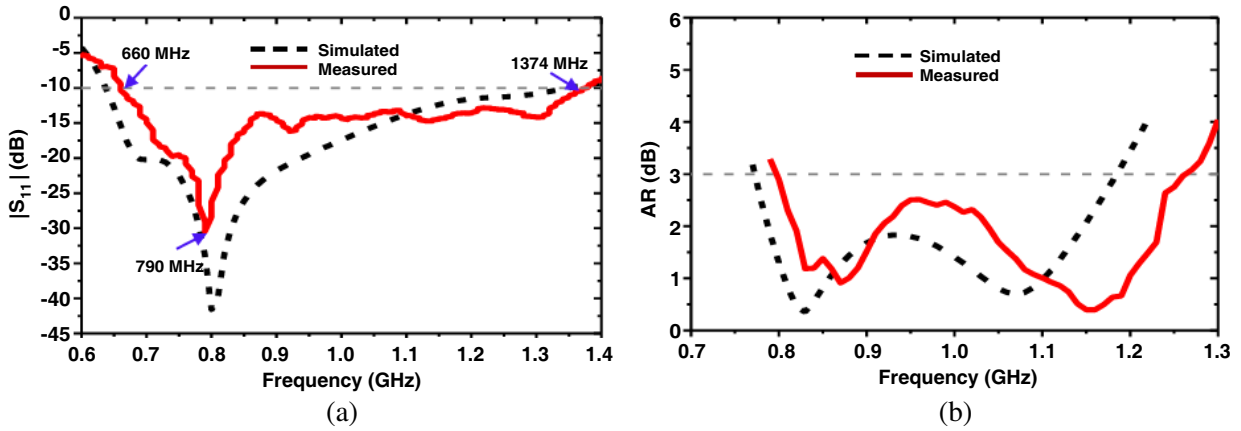


Figure 7. Simulated and measured results of (a) reflection coefficient $|S_{11}|$ and (b) axial ratio of the proposed antenna.

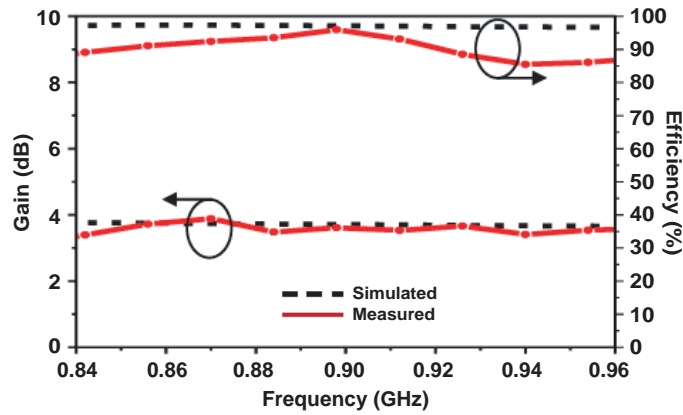


Figure 8. Simulated and measured efficiency and gain across the UHF RFID band for the proposed antenna.

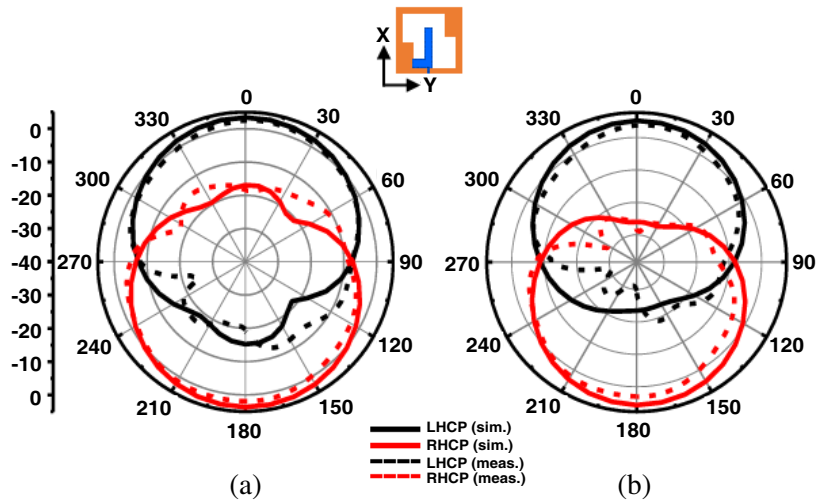


Figure 9. Simulated and measured radiation patterns of the proposed antenna at 900 MHz. (a) x - z plane. (b) y - z plane.

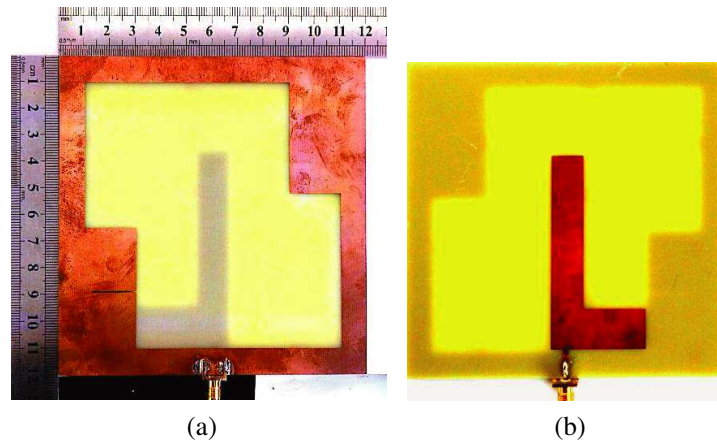


Figure 10. Fabricated proposed antenna. (a) Top view. (b) Bottom view.

to the fabrication tolerance. Apparently, both the simulated and measured impedance bandwidths and axial ratio bandwidths cover the entire UHF RFID band easily. The simulated and measured radiation efficiencies and gains of the proposed antenna are depicted in Figure 8. The antenna exhibits measured gain between 3.3 and 3.9 dBi. The simulated radiation efficiency and gain agree well with the corresponding measured results. Figure 9 shows the simulated and measured radiation patterns at 900 MHz in the XZ and YZ planes, respectively. In both planes, the antenna shows bidirectional radiation characteristics. The simulated and measured results of radiation patterns agree well. The top and bottom views of the fabricated antenna are shown in Figure 10.

A comparison between the proposed antenna and other universal UHF RFID reader antennas is presented in Table 2. It is worth noting that the proposed antenna has a wider impedance bandwidth, wider AR bandwidth, and compact size than other reader antennas in Table 2.

Table 2. Proposed antenna performance comparison.

Ant.	10-reflection coefficient $ S_{11} $ BW (MHz)	3-dB axial ratio BW (MHz)	Max. Gain (dBi)	Dimensions ($L \times W \times H$) mm ³
Ref. [4]	203 760–963	146 818–964	8.3	250 × 250 × 35
Ref. [6]	328 748–1076	165 805–970	3.1	100 × 100 × 13.6
Ref. [9]	380 618–998	332 791–1123	3.4	120 × 120 × 0.8
Ref. [10]	142 860–1002	166 857–1023	6.8	126 × 121 × 0.8
Ref. [11]	394 772–1166	125 840–965	2.9	100 × 100 × 1.6
Proposed	714 660–1374	473 796–1269	3.9	120 × 120 × 1.6

4. CONCLUSION

In this paper, a compact wideband CP slot antenna is proposed for universal UHF RFID reader applications, fabricated and tested. By using a square slot with two rectangular stubs placed at opposite corners and an L-shaped strip radiator, the antenna has obtained desired performances of reflection coefficient, axial ratio, gain, radiation efficiency, and radiation patterns over the entire UHF RFID band (840–960 MHz). The proposed antenna has a measured < 10 -dB reflection coefficient bandwidth of 70.2% (660–1374 MHz), measured 3-dB AR bandwidth of 45.8% (796–1269 MHz), and maximum measured gain of 3.9 dBi. The measurement results agree well with the corresponding simulated ones. The structure of the proposed antenna is simple and easy for design and fabrication. The proposed antenna has several advantages such as a dual circular polarization characteristic, very wide impedance bandwidth, very wide AR bandwidth, a planar single-layer structure, and compact size. Therefore, it is a good candidate for UHF RFID reader applications.

REFERENCES

1. Liu, Q., J. Shen, J. Yin, H. Liu, and Y. Liu, "Compact 0.92/2.45-GHz dual-band directional circularly polarized microstrip antenna for handheld RFID reader applications," *IEEE Transactions on Antennas and Propagation*, Vol. 63, 3849–3856, 2015.
2. Ismail, I. and S. Norzeli, "UHF RFID reader antenna with high gain," *International Journal of Electrical and Electronics System Research*, Vol. 6, 46–52, 2013.
3. Farswan, A., A. K. Gautam, B. K. Kanaujia, and K. Rambabu, "Design of Koch fractal circularly polarized antenna for handheld UHF RFID reader applications," *IEEE Transactions on Antennas and Propagation*, Vol. 64, 771–775, 2016.
4. Chen, Z. N., X. Qing, and H. L. Chung, "A universal UHF RFID reader antenna," *IEEE Transactions on Microwave Theory and Techniques*, Vol. 57, 1275–1282, 2009.
5. Chen, W.-S. and Y.-C. Huang, "A novel CP antenna for UHF RFID handheld reader," *IEEE Antennas and Propagation Magazine*, Vol. 55, No. 4, 128–137, 2013.
6. Liu, Q., J. Shen, H. Liu, Y. Wu, M. Su, and Y. Liu, "Low-cost compact circularly polarized directional antenna for universal UHF RFID handheld reader applications," *IEEE Antennas and Wireless Propagation Letters*, Vol. 14, 1326–1329, 2015.
7. Liu, X., Y. Liu, and M. M. Tentzeris, "A novel circularly polarized antenna with coin-shaped patches and a ring-shaped strip for worldwide UHF RFID applications," *IEEE Antennas and Wireless Propagation Letters*, Vol. 14, 707–710, 2015.
8. Wang, Z., et al., "Single-fed broadband circularly polarized stacked patch antenna with horizontally meandered strip for universal UHF RFID applications," *IEEE Transactions on Microwave Theory and Techniques*, Vol. 59, No. 4, 1066–1073, 2011.
9. Cao, R. and S.-C. Yu, "Wideband compact CPW-fed circularly polarized antenna for universal UHF RFID reader," *IEEE Transactions on Antennas and Propagation*, Vol. 63, 4148–4151, 2015.
10. Lu, J.-H. and S.-F. Wang, "Planar broadband circularly polarized antenna with square slot for UHF RFID reader," *IEEE Transactions on Antennas and Propagation*, Vol. 61, 45–53, 2013.
11. Xu, B., S. Zhang, Y. Liu, J. Hu, and S. He, "Compact broadband circularly polarised slot antenna for universal UHF RFID readers," *Electronics Letters*, Vol. 51, 808–809, 2015.